

Common features of nanoscale structural correlations in magnetoresistive manganites with ferromagnetic low-temperature state

V. Kiryukhin¹, T. Y. Koo¹, A. Borissov¹, Y. J. Kim², C. S. Nelson², J. P. Hill², D. Gibbs², and S-W. Cheong^{1,3}

(1) *Department of Physics and Astronomy, Rutgers University, Piscataway, New Jersey 08854*

(2) *Department of Physics, Brookhaven National Laboratory, Upton, New York 11973*

(3) *Bell Laboratories, Lucent Technologies, Murray Hill, New Jersey 07974*

(February 1, 2008)

We report x-ray scattering studies of nanoscale structural correlations in $\text{Nd}_{1-x}\text{Sr}_x\text{MnO}_3$ and $\text{La}_{1-x}(\text{Ca,Sr})_x\text{MnO}_3$, $x=0.2-0.5$. We find that the correlated regions possess a temperature-independent correlation length of 2-3 lattice constants which is the same in all samples. The period of the lattice modulation of the correlated regions is proportional to the Ca/Sr doping concentration x . Remarkably, the lattice modulation periods of these and several other manganites with a ferromagnetic ground state fall on the same curve when plotted as a function of x . Thus, the structure of the correlated regions in these materials appears to be determined by a single parameter, x . We argue that these observations provide important clues for understanding the Colossal Magnetoresistance phenomenon in manganites.

PACS numbers: 75.30.Vn, 71.38.+i, 71.30.+h

Manganite perovskites of the chemical formula $\text{A}_{1-x}\text{B}_x\text{MnO}_3$ (where A is a rare earth, and B is an alkali earth atom) have recently attracted considerable attention because they exhibit a wide diversity of ground states and a number of interesting phase transitions [1]. Perhaps the most dramatic of these is the magnetic-field-induced insulator-metal transition which is referred to as the Colossal Magnetoresistance (CMR) effect. In its most widely studied form, the CMR effect is the transition from a paramagnetic insulating (PI) to a ferromagnetic metallic (FM) phase. The very large difference between the electrical resistivities of the PI and FM phases lies at the core of the CMR effect, and considerable efforts have been spent in order to explain this difference [1]. The metallic nature of the FM phase was explained in the 1950's in the framework of the double-exchange (DE) mechanism [1] in which the itinerant e_g electrons have their spins aligned with the localized t_{2g} spins of the Mn atoms by virtue of a strong Hund coupling. The DE mechanism, however, does not explain the high resistivity of the PI phase [2]. While recent experimental [3,4] and theoretical [2] work suggests that the enhanced resistivity might in fact result from the presence of small lattice polarons, the anomalously large resistivity of the PI phase still remains largely unexplained.

With the resurgent interest in the manganites in the 1990's, it was realized that the rich behavior of the manganites results from the complex interplay between the charge, spin, lattice, and orbital degrees of freedom [1]. A very important consequence of the competition between the various degrees of freedom is the large variety of inhomogeneous states exhibited by the manganites [5]. The characteristic length scale of these inhomogeneous states varies from microns in conventional phase-separated states down to nanometers in the materials exhibiting nanoscale charge/orbitally ordered re-

gions [1,5-7].

There is a growing body of evidence that the large resistivity of the PI phase in manganites is associated with nanoscale inhomogeneities. In fact, it was recently found that the PI phase exhibits short-range structural correlations [7,8]. It was proposed that these correlations reflect the presence of nanoscale correlated regions possessing local charge/orbital order [7,8]. The associated Jahn-Teller lattice distortions form a periodic lattice modulation in the ordered regions. The electrical resistivity of the PI state has been shown to increase with increasing concentration of these correlated regions [7], suggesting that the large resistivity of this state is due to the presence of such regions. Therefore, understanding the properties of the correlated regions is a necessary step toward understanding the transport properties of the PI phase and the mechanism of the CMR effect.

There is, however, only limited and indirect experimental information about the local structure of the correlated nanoregions. In this work, we report a systematic x-ray diffraction study of the structural correlations in $\text{Nd}_{1-x}\text{Sr}_x\text{MnO}_3$, $x=0.3-0.5$, and $\text{La}_{1-x}(\text{Ca,Sr})_x\text{MnO}_3$, $x=0.2, 0.25$. We find that the correlation length of these regions is the same in all the samples studied and does not depend on temperature. Further, the period of the lattice modulation in the correlated regions was found to vary with Sr/Ca doping concentration x , following an approximately linear relationship with x . Remarkably, the lattice modulation periods of the investigated samples, as well as of several other manganites with a ferromagnetic ground state, fall on the same curve. Thus, the structure of the correlated regions appears to be common to all these materials, and determined by a single parameter, x . These observations impose strict constraints on possible models of the structure of the correlated domains as well as on the mechanism for their formation and should,

therefore, provide important clues for understanding the CMR phenomenon in manganites.

Single crystals of $\text{Nd}_{1-x}\text{Sr}_x\text{MnO}_3$ ($x=0.3, 0.45$, and 0.5), $\text{La}_{0.8}\text{Ca}_{0.2}\text{MnO}_3$, and $\text{La}_{0.75}(\text{Ca}_{0.45}\text{Sr}_{0.55})_{0.25}\text{MnO}_3$ were grown using the floating zone technique. X-ray diffraction measurements were carried out at beamlines X22C and X20C at the National Synchrotron Light Source. A 10 keV x-ray beam was focused by a mirror, monochromatized by a double-crystal Ge (111) monochromator, scattered from the sample, and analyzed with a pyrolytic graphite crystal. The samples were mounted in a closed-cycle refrigerator ($T=10\text{--}450$ K). In this paper, Bragg peaks are indexed in the orthorhombic $Pbnm$ notation in which the longest lattice constant is c , and scattering vectors (h, k, l) are given in reciprocal lattice units.

We first focus our discussion on the properties of the $\text{Nd}_{1-x}\text{Sr}_x\text{MnO}_3$ samples with $x=0.3\text{--}0.5$. These are paramagnetic insulators at high temperatures. With decreasing temperature, they undergo a transition to a ferromagnetic metallic state at $T_c \approx 210$ K, 280 K, and 250 K for $x=0.3, 0.45$, and 0.5 , respectively [9]. In addition, the $x=0.5$ sample undergoes a transition to a CE-type charge-ordered state at $T_{co}=150$ K. Fig. 1 shows that in the PI phase, all these samples exhibit broad peaks in scans taken along the b^* direction in reciprocal space. These broad peaks arise due to the presence of correlated nanoregions [7]. The intensity of these peaks reflects the concentration of the correlated regions [10], the peak width is inversely proportional to their size (correlation length), and the peak position defines the period of the lattice modulation in the correlated regions. The peaks are observed on top of a sloping background which is attributed to scattering from uncorrelated polarons, also known as Huang scattering, and to thermal-diffuse scattering [4]. The overall scattering pattern is illustrated in Fig 2, which shows a contour plot of the x-ray intensity in the $x=0.3$ sample at $T=230$ K around the $(4, 4, 0)$ Bragg peak. In this figure, two broad peaks at $(4.5, 4, 0)$ and $(4, 4.5, 0)$ are superimposed on a “butterfly-like” shaped background which is characteristic of single-polaron scattering in the manganites [4]. The broad peaks are observed along both the a and b crystallographic directions. However, it is not possible to establish with any certainty whether this is because there are two different modulation vectors present or merely arises from crystallographic twinning in the sample.

The data of Fig. 1, and subsequent data taken as a function of temperature, were fitted to a sum of a Gaussian line shape and a monotonically sloping background, the latter described by a power-law function. Several other descriptions were also tried, but the resulting parameters were not found to be significantly different. The error bars in the figures reflect the total parameter variation, including that due to different possible fitting functions.

Fig. 3(a) shows the intensity of the correlated peaks in the $x=0.3$ and 0.5 samples as a function of temperature (the $x=0.45$ data are omitted for clarity). As previously found in $\text{La}_{0.7}\text{Ca}_{0.3}\text{MnO}_3$ [7], this intensity is strongly reduced in the ferromagnetic metallic phase. However, the structural correlations do not completely disappear below the Curie temperature, and in the $x=0.3$ sample small concentrations of the correlated regions survive in the FM region of the phase diagram even at the lowest temperatures. This observation is consistent with the results of neutron measurements of the pair-distribution function in related samples [11]. These latter measurements showed that local Jahn-Teller lattice distortions, albeit in small concentrations, are still present in the FM phase. Our data demonstrate that at least some of these distortions stem from the correlated regions discussed in this work.

The strong reduction of the correlations below T_c is consistent with a picture in which the e_g electrons in the correlated regions are localized: as these regions disappear, the resistivity decreases. While the correlations are suppressed below T_c in all our samples, the transition in the $x=0.3$ sample is much sharper than that in the $x=0.5$ sample. This observation is in general agreement with recent reports of anisotropy and possible inhomogeneity of the FM state in $\text{Nd}_{0.5}\text{Sr}_{0.5}\text{MnO}_3$ [12].

$\text{La}_{0.8}\text{Ca}_{0.2}\text{MnO}_3$ and $\text{La}_{0.75}(\text{Ca}_{0.45}\text{Sr}_{0.55})_{0.25}\text{MnO}_3$ samples with $T_c \approx 190$ K and 300 K, respectively, exhibited transport, magnetic, and structural properties similar to those of $\text{Nd}_{1-x}\text{Sr}_x\text{MnO}_3$. Nanoscale structural correlations in these samples were analyzed in the same manner as those of $\text{Nd}_{1-x}\text{Sr}_x\text{MnO}_3$. The results of this analysis are shown in Fig. 4. Figs. 3 and 4 show that the qualitative features of the nanoscale correlations in the $(\text{Nd}, \text{Sr})\text{MnO}_3$ and $(\text{La}, \text{Ca}, \text{Sr})\text{MnO}_3$ samples are very similar.

Figs. 3(b) and 4(b) show the correlation length of the ordered regions. The correlation length is defined as the inverse half-width-at-half-maximum of the diffraction peak. While this definition gives the correct correlation length for exponentially decaying correlations and Lorentzian line shape, it does not necessarily provide a good measure for the “size” of the ordered regions. For example, simple calculations of the structure factor for perfectly ordered clusters of a finite size show that in this case the correlation length, as defined above, underestimates the cluster size by as much as a factor of two. Therefore, even though the correlation length ξ determined in our experiments is between 2 and 3 lattice constants, the number of three-dimensional unit cells in the ordered regions could be as large as $(2\xi)^3$, *i.e.* about one hundred.

The data of Figs. 3(b), 4(b) show that the size of the correlated regions does not change with temperature and is the same for all the samples, to within errors. This same size was also previously obtained for correlated re-

gions in $\text{La}_{0.7}\text{Ca}_{0.3}\text{MnO}_3$ samples [8]. Taken together, these results suggest that there is a common mechanism defining the size of the correlated regions in these materials.

The period of the lattice modulation in the correlated regions is shown in Figs. 3(c), 4(c). This period is different in different samples. However, as was the case for the correlation length, it is temperature-independent, to within the experimental errors. In Fig. 5, we plot the period of the lattice modulation as a function of doping, x . We also show results of previous measurements in $\text{La}_{0.8}\text{Ca}_{0.2}\text{MnO}_3$, $\text{La}_{0.7}\text{Ca}_{0.3}\text{MnO}_3$, and $(\text{Sm}_{0.875}\text{Nd}_{0.125})_{0.52}\text{Sr}_{0.48}\text{MnO}_3$ samples from Refs. [7], [8], and [4] which all have FM ground states. Remarkably, all the results shown in Fig. 5 appear to fall on the same curve. This observation, together with the independence of the nanoregion size on temperature and sample composition, strongly suggests that the structure of the correlated regions in these compounds is defined by a single parameter, x .

These observations impose constraints on any possible models for the structure of the correlated regions, as well as on the mechanism responsible for their formation. In particular, they indicate that the mechanism controlling the period of the lattice modulation in these regions acts via the Ca/Sr doping concentration x in the sample. In the first approximation, the carrier concentration in the samples is proportional to x , and therefore the carrier concentration might, in fact, be the parameter defining the structure of the correlated regions. In addition, there appears to be a common mechanism defining the size of the correlated regions in these materials. While such a mechanism is currently unknown, we would like to make several comments on the possible structure of the ordered regions. First, because of the characteristic lattice distortion and the insulating properties of the correlated regions, it is likely that they possess charge and orbital order. Moreover, for $x=0.3$, the lattice modulation has the same wave vector as the CE-type charge/orbitally ordered state. For $x=0.3$, therefore, it is reasonable to assume that the correlated regions are in fact small domains possessing the CE-type order with its checker-board-type charge order and the characteristic orbital ordering [1]. As x grows, different charge/orbitally ordered structures, possibly containing discommensurations [1], may be realized. Finally, as x approaches 0.5, the period of the lattice modulation approaches 3, and one of the “striped” structures observed in highly doped-manganites [1] could be realized. As discussed above, the small correlation lengths observed in our experiments are compatible with all these structures.

If the above scenario is correct, one has to explain why the proposed charge-ordered structures are observed at doping levels different from those of the corresponding long-range ordered counterparts. The CE-type order, for example, is most stable at $x=0.5$, and the striped

structure with a period of 3 is observed at $x=2/3$ (see grey symbols in Fig. 5). One possible reason for this discrepancy might be the nanoscale phase separation in which charge-rich and charge-poor regions are formed. It is possible that the charge concentration in the charge-depleted correlated regions corresponds to the ideal concentration required for the formation of the charge-ordered structures with the observed periodicity. Such variations in the charge concentration could result from nanoscale chemical inhomogeneities, such as clustering of the cations in the A-position. This scenario would naturally explain the independence on temperature of the correlation length and the modulation wavevector in the correlated regions, but does not provide any straightforward explanation for the observed dependence of the modulation wavevector on the sample composition.

Even in the absence of chemical inhomogeneities, however, formation of charge-rich and charge-poor regions is still possible. A number of theoretical calculations, in fact, predict such a phase separation [5], and some experimental evidence has recently become available [13]. Note, this nanoscale phase separation is different from the well-known case of phase separation in the manganites, in which domains with sub-micrometer size are formed [5]. In the latter case, Coulomb forces prevent any significant charge redistribution. The Coulomb forces should not, however, prevent the formation of nanoscale charge-depleted regions. They can, nevertheless, be one of the factors limiting the region size. Of course, other mechanisms explaining the experimental observations are possible. For example, nesting properties of the Fermi surface have been proposed for the origin of the structural correlations observed in two-dimensional manganites [14]. However, preliminary calculations suggest that this scenario is unlikely in the three-dimensional manganites discussed here [15]. In another recent work [16], effects of quenched disorder are considered, but detailed predictions about the structure of the PI state are yet to be achieved. Clearly, further work is needed to establish the actual mechanism leading to the formation of the correlated regions.

Finally, we would like to emphasize that all of the samples considered above exhibit the FM phase at low temperatures (the exception is $\text{Nd}_{0.5}\text{Sr}_{0.5}\text{MnO}_3$, in which the lowest-temperature charge-ordered state is separated from the PI phase by the intermediate-temperature FM state). The case of the transition from the PI or FM phase directly to the charge-ordered phase, such as in $\text{Pr}_{1-x}\text{Ca}_x\text{MnO}_3$ or $\text{La}_{0.5}\text{Ca}_{0.5}\text{MnO}_3$, is more complex. In such transitions, the periodicity of the lattice modulation and the correlation length vary on warming as the low-temperature, long-range charge order disappears and the high-temperature correlations arise [8,17]. The existing experimental data are not completely consistent, and it is unclear as to what extent they reflect the intrinsic properties of the PI state. Systematic measurements at

temperatures much larger than the charge-ordering transition temperature are needed to answer this question.

In summary, we report that the nanoscale structural correlations characteristic of the paramagnetic state of magnetoresistive manganites possess a common correlation length and that the structure of the correlated regions appears to be determined by a single parameter – the concentration of the doped divalent ions. We argue that observation of such common features imposes strict constraints on the possible mechanism responsible for the formation of the correlated regions, and therefore should provide important clues for understanding the CMR mechanism in manganites.

We are grateful to A. J. Millis for important discussions. This work was supported by the NSF under grants No. DMR-0093143, DMR-9802513, by the DOE under contract No. AC02-98CH10886, and by the NSF MR-SEC program, Grant No. DMR-0080008.

-
- [1] For a review, see *Colossal Magnetoresistance Oxides*, edited by Y. Tokura (Gordon & Breach, London, 1999)
 - [2] A. J. Millis, P. B. Littlewood, and B. I. Shraiman, Phys. Rev. Lett. **74**, 5144 (1995); A. Alexandrov and A. M. Bratkovsky, *ibid.* **82**, 141 (1999)
 - [3] S. J. L. Billinge, R. G. DiFrancesco, G. H. Kwei, J. J. Neumeier, and J. D. Thompson, Phys. Rev. Lett. **77**, 715 (1996); C. H. Booth, F. Bridges, G. H. Kwei, J. M. Lawrence, A. L. Cornelius, and J. J. Neumeier, *ibid.* **80**, 853 (1998); K. H. Kim, J. Y. Gu, H. S. Choi, G. W. Park, and T. W. Noh, *ibid.* **77**, 1877 (1996); M. Jaime, H. T. Hardner, M. B. Salamon, M. Rubinstein, P. Dorsey, and D. Emin, *ibid.* **78**, 951 (1997); A. Machida, Y. Moritomo, and A. Nakamura, Phys. Rev. B **58**, R4281 (1998)
 - [4] S. Shimomura, N. Wakabayashi, H. Kuwahara, and Y. Tokura, Phys. Rev. Lett. **83**, 4389 (1999); L. Vasiliu-Doloc, S. Rosenkranz, R. Osborn, S. K. Sinha, J. W. Lynn, J. Mesot, O. H. Seeck, G. Preosti, A. J. Fedro, and J. F. Mitchell, *ibid.* **83**, 4393 (1999)
 - [5] For a review, see E. Dagotto, T. Hotta, and A. Moreo, Phys. Rep. **344**, 1 (2001)
 - [6] V. Podzorov, B. G. Kim, V. Kiryukhin, M. E. Gershenson, and S-W. Cheong, Phys. Rev. B **64**, 140406 (2001)
 - [7] P. Dai, J. A. Fernandez-Baca, N. Wakabayashi, E. W. Plummer, Y. Tomioka, and Y. Tokura, Phys. Rev. Lett. **85**, 2553 (2000); C. P. Adams, J. W. Lynn, Y. M. Mukovskii, A. A. Arsenov, and D. A. Shulyatev, *ibid.* **85**, 3954 (2000);
 - [8] C. S. Nelson, M. v. Zimmermann, Y. J. Kim, J. P. Hill, Doon Gibbs, V. Kiryukhin, T. Y. Koo, S-W. Cheong, D. Casa, B. Keimer, Y. Tomioka, Y. Tokura, T. Gog, and C. T. Venkataraman, Phys. Rev. B **64**, 174405 (2001)
 - [9] R. Kajimoto, H. Yoshizawa, H. Kawano, H. Kuwahara, Y. Tokura, K. Ohoyama, and M. Ohashi, Phys. Rev. B **60**, 9506 (1999)

- [10] This intensity can also reflect the amplitude of the lattice modulation in the correlated regions. In principle, this can change with temperature. However, this scenario appears to be inconsistent with the results of the neutron measurements of Ref. [11]
- [11] D. Louca, T. Egami, E. L. Brosha, H. Röder, and A. R. Bishop, Phys. Rev. B **56**, R8475 (1997)
- [12] H. Yoshizawa, R. Kajimoto, H. Kawano, J. A. Fernandez-Baca, Y. Tomioka, H. Kuwahara, and Y. Tokura, Mater. Sci. Eng. B, **B63**, 125 (1999); V. Kiryukhin, B. G. Kim, T. Katsufuji, J. P. Hill, and S-W. Cheong, Phys. Rev. B **63**, 144406 (2001)
- [13] J. Alonso, A. Arroyo, J. M. González-Calbet, M. Vallet-Regí, J. L. Martinez, J. M. Rojo, and A. Hernando, Phys. Rev. B **64**, 172410 (2001)
- [14] Y.-D. Chuang, A. D. Gromko, D. S. Dessau, T. Kimura, and Y. Tokura, Science **292**, 1509 (2001); see also B. J. Campbell, R. Osborn, D. N. Argytiou, L. Vasiliu-Doloc, J. F. Mitchell, S. K. Sinha, U. Ruett, C. D. Ling, Z. Islam, and J. W. Lynn, cond-mat/0106477 (unpublished)
- [15] A. J. Millis, private communication
- [16] J. Burgy, M. Mayr, V. Martin-Mayor, A. Moreo, and E. Dagotto, cond-mat/0107300 (unpublished)
- [17] C. H. Chen, S. Mori, and S-W. Cheong, Phys. Rev. Lett. **83**, 4792 (1999); S. Shimomura, T. Tonegawa, K. Tajima, N. Wakabayashi, N. Ikeda, T. Shobu, Y. Noda, Y. Tomioka, and Y. Tokura, Phys. Rev. B **62**, 3875 (2000); R. Kajimoto, H. Yoshizawa, Y. Tomioka, and Y. Tokura *ibid.* **63**, 212407 (2001)
- [18] C. H. Chen, S-W. Cheong, and H. Y. Hwang, J. Appl. Phys. **81**, 4326 (1997)

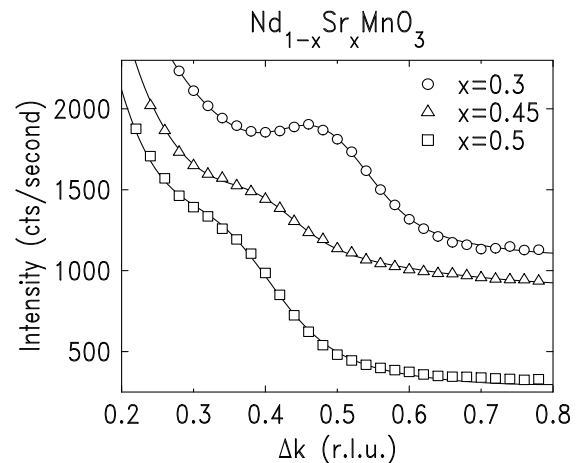


FIG. 1. X-ray scans along the $(4, 6+\Delta k, 0)$ direction ($\text{Nd}_{0.55}\text{Sr}_{0.45}\text{MnO}_3$ and $\text{Nd}_{0.5}\text{Sr}_{0.5}\text{MnO}_3$), and the $(4, 4+\Delta k, 0)$ direction ($\text{Nd}_{0.7}\text{Sr}_{0.3}\text{MnO}_3$). The temperatures are 210 K, 275 K, and 260 K for the $x=0.3$, 0.45, and 0.5 samples, respectively. The solid lines are the results of fits, as discussed in the text. For clarity, $x=0.3$ and $x=0.45$ data are shifted up by 750 cts/second.

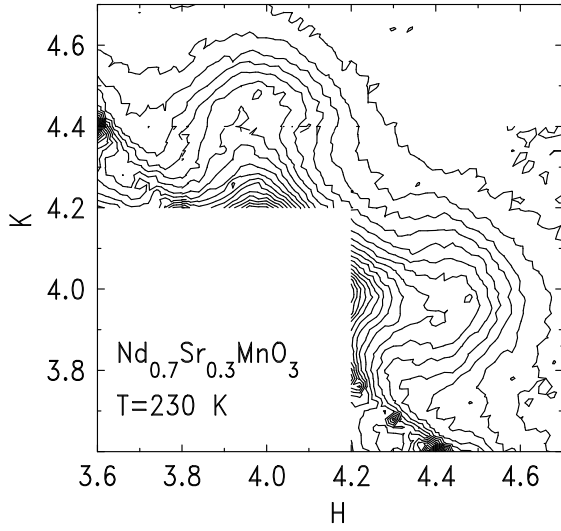


FIG. 2. Contour plot of the x-ray intensity around the (4, 4, 0) Bragg peak at $T=230$ K in $\text{Nd}_{0.7}\text{Sr}_{0.3}\text{MnO}_3$.

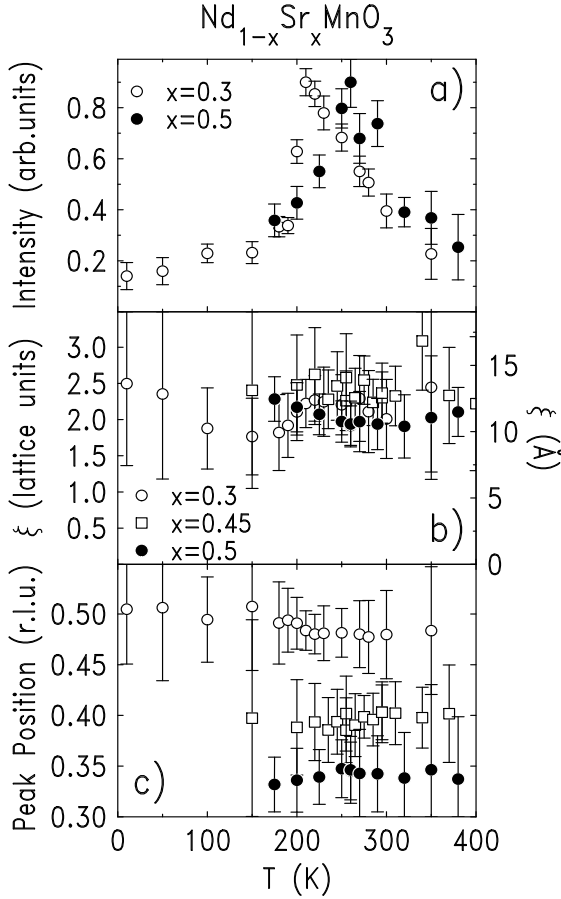


FIG. 3. (a) Temperature dependence of the intensity of the peak due to the structural correlations in $\text{Nd}_{1-x}\text{Sr}_x\text{MnO}_3$. The single-polaron background is subtracted as discussed in the text. (b) The correlation length of the ordered regions. (c) The position of the peak relative to the nearest Bragg peak (the lattice modulation wave vector).

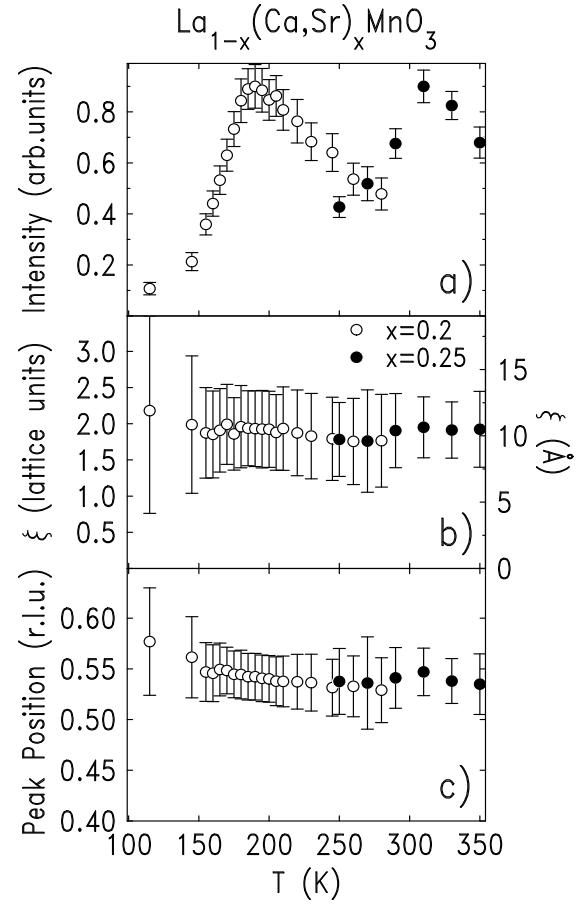


FIG. 4. (a) Temperature dependence of the intensity of the peak due to the structural correlations in $\text{La}_{0.8}\text{Ca}_{0.2}\text{MnO}_3$, and $\text{La}_{0.75}(\text{Ca}_{0.45}\text{Sr}_{0.55})_{0.25}\text{MnO}_3$. The single-polaron background is subtracted as discussed in the text. (b) The correlation length of the ordered regions. (c) The position of the peak relative to the nearest Bragg peak (the lattice modulation wave vector).

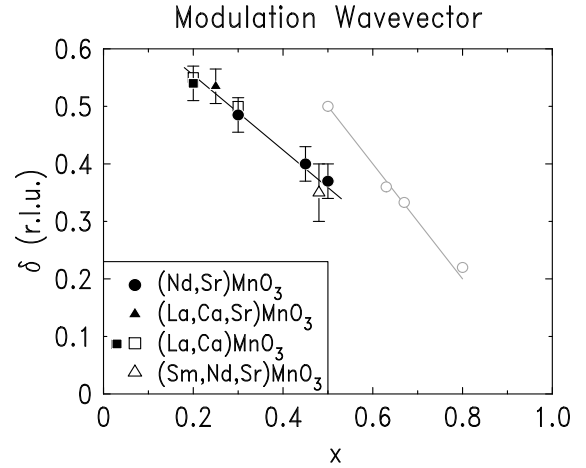


FIG. 5. The wave vector δ of the lattice modulation in the correlated regions as a function of doping x (black symbols). Filled symbols represent our own data. The data shown with open symbols were taken from Refs. [4,7,8]. Grey symbols show the wave vector of the structures with *long-range* charge/orbital order observed in manganites with $x > 0.5$ (Ref. [18]).